Journal of Comparative Physiology B (2020) 190:219–230
https://doi.org/10.1007/s00360-020-01260-x

ORIGINAL PAPER

Salinity-dependent expression of *ncc2* in opercular epithelium and gill of mummichog (*Fundulus heteroclitus*)

Jason P. Breves[1] · Julie A. Starling[2] · Christine M. Popovski[1] · James M. Doud[1] · Christian K. Tipsmark[2]

Received: 20 May 2019 / Revised: 20 December 2019 / Accepted: 9 January 2020 / Published online: 24 January 2020

Abstract

Mummichogs (*Fundulus heteroclitus*) can tolerate abrupt changes in environmental salinity because of their ability to rapidly adjust the activities of ionocytes in branchial and opercular epithelia. In turn, the concerted expression of sub-cellular effectors of ion transport underlies adaptive responses to fluctuating salinities. Exposure to seawater (SW) stimulates the expression of $Na^+/K^+/2Cl^-$ *cotransporter 1* (*nkcc1*) and *cystic fibrosis transmembrane regulator* (*cftr*) mRNAs in support of ion extrusion by SW-type ionocytes. Given the incomplete understanding of how freshwater (FW)-type ionocytes actually operate in mummichogs, the transcriptional responses essential for ion absorption in FW environments remain unresolved. In a subset of species, a 'fish-specific' Na^+/Cl^- cotransporter denoted Ncc2 (Slc12a10) is responsible for the uptake of Na^+ and Cl^- across the apical surface of FW-type ionocytes. In the current study, we identified an *ncc2* transcript that is highly expressed in gill filaments and opercular epithelium of FW-acclimated mummichogs. Within 1 day of transfer from SW to FW, *ncc2* levels in both tissues increased in parallel with reductions in *nkcc1* and *cftr*. Conversely, mummichogs transferred from FW to SW exhibited marked reductions in *ncc2* concurrent with increases in *nkcc1* and *cftr*. Immunohistochemical analyses employing a homologous antibody revealed apical Ncc2-immunoreactivity in Na^+/K^+-ATPase-immunoreactive ionocytes of FW-acclimated animals. Our combined observations suggest that Ncc2/*ncc2*-expressing ionocytes support the capacity of mummichogs to inhabit FW environments.

Keywords Na^+/Cl^- cotransporter · Atlantic killifish · Opercular epithelium · Gill · Ionocyte

Introduction

Fewer than 10% of teleosts are considered euryhaline and can maintain osmotic and ionic homeostasis when exposed to environmental salinities ranging from freshwater (FW) to full-strength seawater (SW) (Schultz and McCormick 2013). The physiological systems supporting euryhalinity enable these species to seek waters suitable for particular life history stages, or, in some instances, to thrive under highly dynamic conditions. Mummichogs (*Fundulus heteroclitus* L. 1766) are native to the east coast of North America where they inhabit tide pools, rivers, and estuaries subjected to tidally driven changes in salinity. Mummichogs can tolerate salinities ranging from FW to hypersaline SW (120‰) (Griffith 1974). This tolerance to a broad range of environmental salinities permits various aspects of their life history, including movements supporting food acquisition and reproduction (Able 2002; Burnett et al. 2007). Thus, as a model system, mummichogs support reductive approaches aimed at identifying the mechanisms of environmental adaptation and ecological specialization (Whitehead 2010; Brennan et al. 2015); this is especially true with respect to characterizing the molecular and cellular mechanisms underlying ionoregulation.

Euryhaline fishes tolerate changes in environmental salinity through the functional coordination of multiple tissues, including the gill, intestine, kidney, and urinary bladder; nonetheless, branchial epithelium is the primary site of Na^+ and Cl^- transport by specialized ionocytes (Marshall and Grosell 2006). In mummichogs, the opercular epithelium also harbors a rich population of ionocytes that

Communicated by B. Pelster.

✉ Jason P. Breves
jbreves@skidmore.edu

[1] Department of Biology, Skidmore College, 815 N. Broadway, Saratoga Springs, NY 12866, USA

[2] Department of Biological Sciences, University of Arkansas, Fayetteville, AK 72701, USA

participates in ionoregulation (Marshall et al. 1997), albeit the contribution of this ionocyte population to sustaining systemic Na^+ and Cl^- balance is seemingly minor (Wood and Laurent 2003; Dymowska et al. 2012). The well-established paradigm for ion secretion by 'SW-type' ionocytes includes the operation of Na^+/K^+-ATPase (Nka) and $Na^+/K^+/2Cl^-$ cotransporter 1 (Nkcc1) in the basolateral membrane and cystic fibrosis transmembrane conductance regulator (Cftr) in the apical membrane (Marshall and Grosell 2006). Alternatively, several models have been presented that describe how 'FW-type' ionocytes absorb ions from dilute environments. These varying models reflect, in part, the evolution of multiple strategies for ion uptake from FW habitats with varying compositions (Dymowska et al. 2012; Takei et al. 2014; Yan and Hwang 2019). Ionocytes are remarkably plastic with respect to how genes encoding sub-cellular effectors of ion transport are expressed during salinity acclimation (Scott et al. 2004; Fiol and Kültz 2007). In turn, insight into the transcriptional responses that support ion uptake by branchial and opercular epithelia can be gained by studying mummichogs undergoing FW-acclimation (Scott et al. 2004, 2005; Brennan et al. 2015).

In a landmark study, Hiroi et al. (2008) revealed that Mozambique tilapia (*Oreochromis mossambicus*) express a 'fish-specific' Na^+/Cl^- cotransporter (Ncc) in the apical membrane of ionocytes abundant in FW-acclimated animals. This 'fish-specific' Ncc is denoted Ncc2 (Slc12a10) and is not a member of the 'conventional' Ncc1 (Slc12a3) clade (Takei et al. 2014). The sub-population of ionocytes that express Ncc2 in tilapia ('Type-II' ionocytes or 'Ncc-cells') leverages Ncc2 for the transport of Na^+ and Cl^- from FW into the ionocyte interior. It was subsequently established that stenohaline zebrafish (*Danio rerio*) likewise employ Ncc2 (Slc12a10.2)-mediated ion uptake (Wang et al. 2009). Accordingly, *ncc2* mRNA levels are markedly increased when tilapia and zebrafish acclimate to low salt conditions such as FW or ion-poor water, respectively (Hiroi et al. 2008; Wang et al. 2009). In a survey of histological observations made on FW-type ionocytes, Hiroi and McCormick (2012) argued for additional instances of Ncc2-mediated ion uptake beyond tilapia and zebrafish, but still within the teleost clade, including Acanthopterygii (the suborder to which mummichogs belong). Moreover, Katoh et al. (2008) and Marshall et al. (2017) reported apical immunoreactivity in FW gill and opercular epithelium of mummichogs using the human T4 antibody that recognizes teleost Nkcc and Ncc proteins (Lytle et al. 1995). In both cases, they observed apical T4-immunoreactivity that is a hallmark of Ncc2-expressing ionocytes (Hiroi and McCormick 2012). In the current study, our objective was to determine whether Ncc2-expressing ionocytes within opercular and branchial epithelia contribute to salinity acclimation by mummichogs. We focused on the 'fish-specific' Ncc2 because expression of the 'conventional' Ncc1 is restricted to the kidney and urinary bladder of teleosts (Kato et al. 2011; Takei et al. 2014). We initially characterized *ncc2* gene expression patterns in steady-state animals as well as animals abruptly transferred to either FW or SW conditions. We then analyzed protein abundance with Western blotting and made immunohistochemical observations of opercular epithelium using an antibody against mummichog Ncc2.

Materials and methods

Experimental animals and rearing conditions

Adult mummichogs of both sexes were collected from an estuary in Avery Point, CT, USA, by seine net and transported to the Skidmore College Animal Care Facility. Fish were maintained in artificial SW (35‰ Instant Ocean, Blacksburg, VA) or FW (5.31 mM Na^+, 5.25 mM Cl^-, 0.10 mM Ca^{2+}) in recirculating stock tanks with particle and charcoal filtration and continuous aeration at 24–27 °C under 12L:12D. Fish were fed Omega One mini pellets (Omega Sea, Painesville, OH) twice daily. All housing and experimental procedures were approved by the Institutional Animal Care and Use Committee (IACUC) of Skidmore College. Fish for Western blot analysis were obtained from Aquatic Research Organisms, Inc. (Hampton, NH) and held in FW or SW. Handling and experimental procedures were approved by the IACUC of the University of Arkansas.

Tissue and steady-state expression of *ncc2* mRNA

Tissues were collected from mummichogs maintained in FW for > 1 year ($n = 4$–6). Fish were lethally anesthetized with 2-phenoxyethanol (2-PE; 2 ml/l, Sigma-Aldrich, St. Louis, MO) and the following tissues were collected: whole brain, opercular epithelium, gill, liver, body kidney, heart, muscle, fat, anterior intestine, and skin. Tissues were stored in TRI Reagent (MRC, Cincinnati, OH) at − 80 °C until RNA isolation. To compare *ncc2*, *nkcc1*, and *cftr* mRNA levels between SW- and FW-acclimated animals ($n = 6$), opercular epithelium and gill filaments were collected from animals acclimated to the two environmental salinities for > 1 month.

Effect of salinity transfer (SW to FW and FW to SW) on gene expression in opercular epithelium and gill

The first transfer experiment entailed the abrupt transfer of mummichogs from SW to FW. At the time of transfer (0 h), fish were quickly netted from a SW stock tank and distributed into six recirculating 38-l tanks ($n = 6$–8 fish/tank), three tanks containing FW and three tanks containing SW (time-matched controls). Time 0 fish were sampled

directly from the SW stock tank. Fish were fasted for the duration of the experiment. At the time of sampling (1, 3, and 7 days after transfer), all the fish housed in one FW and one SW tank were netted and anesthetized with a lethal dose of 2-PE (2 ml/l). Fish were then rapidly decapitated and the opercular epithelium and gill filaments were excised and stored in TRI Reagent at − 80 °C until tissue homogenization and RNA isolation. White muscle was collected from the caudal musculature and the water content was measured gravimetrically after drying overnight at 90 °C. This procedure provides a measure of body hydration levels, which we predict would change if animals were not successfully acclimating to changes in salinity. For the second transfer experiment, mummichogs held in a FW stock tank were abruptly transferred to six recirculating tanks ($n = 6$–8 fish/tank); three tanks contained SW and three tanks contained FW (time-matched controls). Fish were sampled at 1, 3, and 7 days after transfer as described above. Time 0 fish were sampled directly from the FW stock tank.

Ncc sequences and phylogenetic analysis

'Conventional' *ncc* (*ncc1*, *slc12a3*) and 'fish-specific' *ncc* (*ncc2*, *slc12a10*) mRNA sequences were identified in the mummichog database in GenBank (Benson et al. 2000) by using BLAST similarity search (Altschul et al. 1997) with known teleost *slc12a3* and *slc12a10* paralogs from the zebrafish and medaka genomes as search parameters. Sequences (Acc. No. in parentheses) obtained from GenBank were: mummichog *ncc1* (XM_021318983.1) and mummichog *ncc2* (XM_021310632.1). The naming was verified by phylogenetic analysis (Fig. 1) using the predicted amino acid sequences obtained from GenBank and aligned using the Clustal Omega server at the European Bioinformatics Institute. The phylogenetic tree was constructed using maximum likelihood analysis and included known zebrafish, Japanese medaka, Nile tilapia, Xenopus, canary, and human sequences: zebrafish Ncc1 (NM_001045080.1), zebrafish Ncc2.1 (NM_001161378.1), zebrafish Ncc2.2 (NM_001045001.1), zebrafish Ncc2.3 (NM_001135131.1), medaka Ncc1 (XM_011475726.2), medaka Ncc2.1 (KJ489428.1), medaka Ncc2.2 (KJ489429.1), tilapia Ncc1 (XM_003439377), tilapia Ncc2.1 (XM_019354136), tilapia Ncc2.2 (XM_019354139), tilapia Ncc2.3 (XM_019354135), Xenopus Ncc1 (XP_018113335.1), canary NCC1 (XP_018770179.1), human NCC1 (P55017.3), and human NKCC1 (AAB07364.1) as an outgroup. One thousand bootstraps were used to test the consistency of grouping within the tree. The maximum likelihood majority rule consensus tree was created using SEQBOOT, PROML, and CONSENSE, all programs of the PHYLIP package (Felsenstein 1989).

RNA extraction, cDNA synthesis, and quantitative real-time PCR (qRT-PCR)

Total RNA was extracted from tissues by the TRI Reagent procedure according to the manufacturer's protocol. RNA concentration and purity were assessed by spectrophotometric absorbance (Nanodrop 1000, Thermo Scientific,

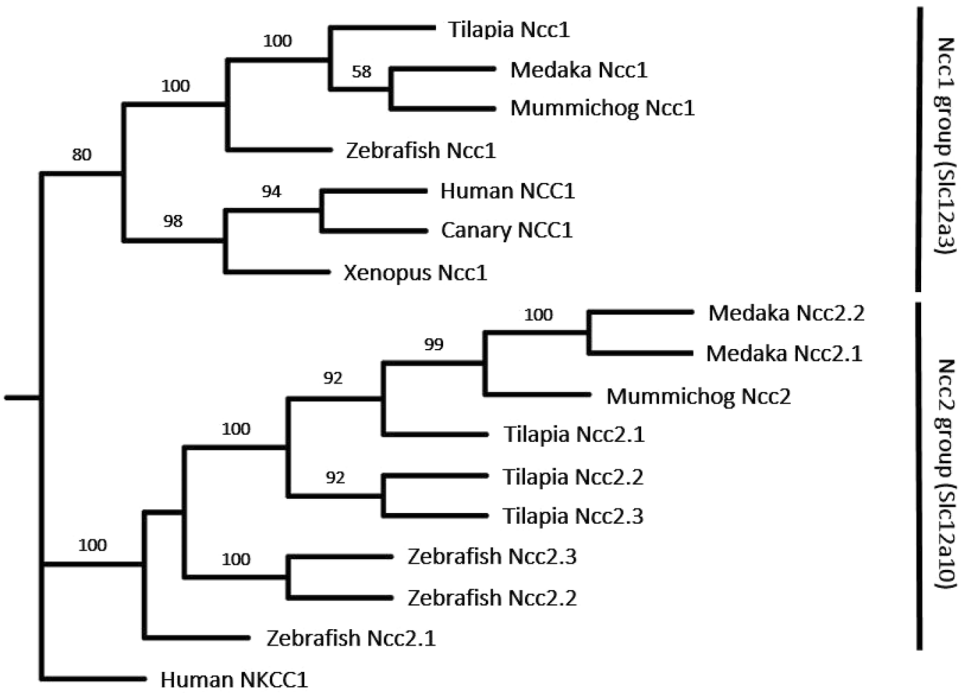

Fig. 1 Phylogenetic analysis of 'conventional' Ncc (Ncc1, Slc12a3) and 'fish-specific' Ncc (Ncc2, Slc12a10) orthologs in select vertebrates. The tree was generated using predicted Ncc1 and Ncc2 amino acid sequences from mummichog, zebrafish, Japanese medaka, Nile tilapia, Xenopus, canary, and human. Human NKCC1 (Slc12a2) was used as an outgroup. The bootstrap consensus tree was inferred from 1000 replicates and values are given in percent

Wilmington, DE). First-strand cDNA was synthesized by reverse transcribing 50–100 ng total RNA with a High Capacity cDNA Reverse Transcription Kit (Life Technologies, Carlsbad, CA). Relative levels of mRNA were determined by qRT-PCR using the StepOnePlus real-time PCR system (Life Technologies). Primer sequences for *ncc2* (XM_021310632.1) were designed using NCBI Primer-BLAST: F: AGTCACATCCTGACCGGAAAC and R: TCACAGGACTGAGACTGGAT (product = 98 bp). Non-specific product amplification and primer-dimer formation were assessed by melt curve analyses and gel electrophoresis. The *nkcc1* and *cftr* primer sets used in this study, and their specificity, have been previously described (Scott et al. 2005). qRT-PCR reactions were performed in a 15 µl volume containing 2X Power SYBR Green PCR Master Mix (Life Technologies), 200 nmol/l of each primer, nuclease-free water, and 1 µl cDNA template. The following cycling parameters were employed: 2 min at 50 °C, 10 min at 95 °C followed by 40 cycles at 95 °C for 15 s and 60 °C for 1 min. After verification that *ef1α* mRNA levels did not vary across treatments, *ef1α* levels were used to normalize target genes (Scott et al. 2005). Reference and target genes were calculated by the relative quantification method with PCR efficiency correction (Pfaffl 2001). Standard curves were prepared from serial dilutions of control opercular epithelium or gill cDNA and included on each plate to calculate the PCR efficiencies for target and normalization gene assays. Relative gene expression ratios between groups are reported as a fold change from controls.

Primary antibodies

A polyclonal antibody was raised in rabbit against a synthetic peptide corresponding to a portion (NEESQDPQEKAPVRC) of mummichog Ncc2. The affinity-purified antibody was produced by GenScript (Piscataway, NJ). To detect Na^+/K^+-ATPase (Nka), we used a monoclonal mouse antibody (a5) obtained from the Developmental Studies Hybridoma Bank, created by the NICHD of the NIH and maintained at The University of Iowa, Department of Biology (Iowa City, IA).

Western blotting analysis

Western blotting was performed as described previously (Tipsmark et al. 2010). Gill filaments and opercular epithelium from SW- and FW-acclimated (2 months) mummichogs were homogenized in chilled SEID buffer (300 mM sucrose, 20 mM Na2-EDTA, 50 mM imidazole, 0.1% sodium deoxycholate, pH 7.3) with protease inhibitor (P8340; Sigma-Aldrich) using a Brinkmann Polytron homogenizer (Westbury, NY). The homogenate was centrifuged at 5000*g* (10 min, 4 °C) and the resulting supernatant was then transferred to a new tube and then centrifuged at 20,000*g* (60 min, 4 °C). The pellet was dissolved in 30 µl SEID buffer. Protein concentration was evaluated using the Bradford assay. Samples for loading were prepared with NuPage LDS sample buffer (Life Technologies) and 50 mM dithiothreitol and denatured on a heat block (10 min, 70 °C). Proteins (2.5 µg) were separated in a 4–12% Bis–Tris gel with 2-(*N*-morpholino)ethanesulfonic acid sodium dodecyl sulfate (MES SDS) running buffer at 200 V for 30 min (Mini Gel Tank, A25977, Life Technologies). After electrophoresis, proteins were immunoblotted onto nitrocellulose membranes (0.2 µm; Invitrogen, Carlsbad, CA) for 60 min at 10 V (Mini Blot Module, B1000) with transfer buffer (12 mM Tris base, 96 mM glycine, 10% methanol). Membranes were blocked with LI-COR Blocking Buffer (LI-COR Biosciences) for 1 h at room temperature. After blocking, membranes were incubated overnight at 4 °C with a cocktail of two primary antibodies (rabbit anti-Ncc2, 1:200, 1.8 µg/ml; mouse anti-beta actin, 1:2000, 0.5 µg/ml) dissolved in LI-COR Blocking Buffer. Following four washes for 5 min with 1 × Tris-buffered saline with Tween 20 (TBST; 20 mM Tris, 140 mM NaCl, 0.1% Tween-20), membranes were incubated with secondary antibodies (IRDye 680LT goat anti-mouse IgG, 1:10,000; IRDye 800CW goat anti-rabbit IgG, 1:20,000; LI-COR Biosciences) for 60 min in the dark at room temperature. Following four 5 min washes in TBST, membranes were air dried and scanned on an infrared imager (Odyssey, LI-COR Biosciences). The band intensities were quantified using the Image Studio v2.0 software (LI-COR Biosciences) and normalized to beta actin. Apparent molecular size was estimated using pre-stained protein standards (Precision Plus Protein All Blue Standards, Bio-Rad, Hercules, CA). In a separate experiment, the ability of antigenic peptide (GenScript) to neutralize binding of the Ncc2 antibody to target protein was validated by preincubating the primary antibody with 400-fold molar excess of peptide overnight at 4 °C prior to incubation of the membrane.

Immunofluorescence microscopy

For whole-mount immunohistochemistry, opercular epithelia (attached to opercular bone) were fixed overnight in 4% paraformaldehyde (PFA) in 0.1 M phosphate-buffered saline (PBS, pH 7.4) at 4 °C. Fixed samples were washed in PBS with 0.2% Triton-X 100 (PBST) and then immersed in blocking solution (PBST containing 2% normal goat serum, 0.1% bovine serum albumin, 0.02% keyhole limpet hemocyanin, 0.01% sodium azide) overnight at 4 °C. After blocking, specimens were incubated overnight at room temperature with anti-Ncc2 (1:50, 7.1 µg/ml) and anti-Nka (1:1000, 0.3 µg/ml) diluted with blocking solution. After several washes with PBST, samples were incubated overnight at room temperature with secondary antibodies labeled

with fluorescents (donkey anti-rabbit IgG labeled with Alexa Fluor 647 and goat anti-mouse IgG labeled with Alexa Fluor 488, Invitrogen) diluted 1:500 with blocking solution. After rinsing with PBST and then PBS, the opercular epithelium from each specimen was dissected from the opercular bone under a dissecting scope and mounted with 75% glycerol on glass slides. Specimens were observed under a confocal laser scanning microscope (Olympus Fluoview 1200, Center Valley, PA). *z*-stack series were taken on fields within the opercular epithelium using a 60 × oil objective, a zoom of 1.0, and optical sections of 0.5 µm. Images were processed using FV10-ASW v4.1 software (Olympus). Opercular epithelia were examined from individuals held in FW for > 2 weeks ($n = 4$). The specificity of the anti-Ncc2 antibody was assessed by preabsorbing the antibody with the synthetic antigen (GenScript) overnight at room temperature. For the preabsorption test, goat anti-rabbit IgG labeled with Alexa Fluor 488 (Invitrogen) was used as the secondary antibody.

Statistics

Multiple group comparisons for the tissue expression of *ncc2* (Fig. 2a) were performed by one-way ANOVA followed by Tukey's HSD test. Significance was set at $P < 0.05$. For a single comparison, a Student's *t* test was employed (Fig. 2b–g) and significant differences are indicated in figures: $^{**}P < 0.01$, and $^{***}P < 0.001$. Transfer experiments (Figs. 3, 4, 5, 6) were analyzed by two-way ANOVA. Significant effects of treatment, time, or an interaction ($P < 0.05$) are indicated in figures: $^{*}P < 0.05$, $^{**}P < 0.01$, and $^{***}P < 0.001$. When a main effect of treatment, or an interaction between treatment and time was detected, post hoc comparisons (Bonferroni's multiple comparisons test) were employed at each time point. Significant differences between groups at a given time point are also indicated in figures: $^{\dagger}P < 0.05$, $^{\dagger\dagger}P < 0.01$, and $^{\dagger\dagger\dagger}P < 0.001$. Western blot data were analyzed by two-way ANOVA. Significant main effects are indicated in Fig. 7b: $^{*}P < 0.05$. All statistical analyses were performed using GraphPad Prism 6 (GraphPad Software, San Diego, CA).

Results

Ncc sequence and phylogenetic analysis

We identified two Ncc paralogs in the mummichog sequence material available in GenBank, one 'conventional' Ncc1 (Slc12a3) and one 'fish-specific' Ncc2 (Slc12a10). The mummichog paralogs were classified according to phylogenetic analysis including previously named Ncc1 and Ncc2 paralogs in zebrafish, Japanese medaka, Nile tilapia, Xenopus, canary, and human (Fig. 1).

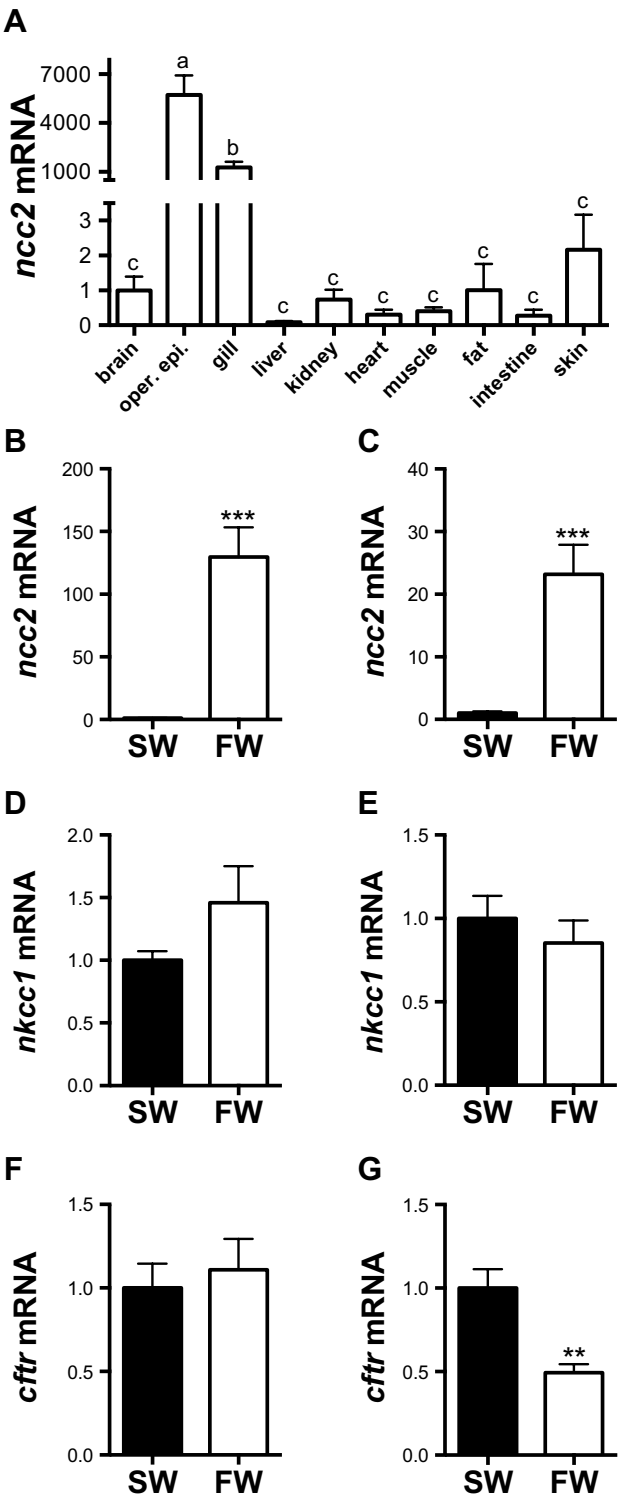

Fig. 2 *ncc2* mRNA levels in various tissues of freshwater (FW)-acclimated mummichogs (**a**). Mean ± SEM ($n = 4$–6). Data were normalized to *ef1α* as a reference gene and are presented relative to brain expression levels. Means not sharing the same letter are significantly different (one-way ANOVA, Tukey's HSD test, $P < 0.05$). *ncc2, nkcc1*, and *cftr* levels in the opercular epithelium (**b**, **d**, **f**) and gill (**c**, **e**, **g**) of seawater (SW)- and FW-acclimated mummichogs ($n = 6$). mRNA levels in FW are presented as a fold change from SW. Asterisks indicate significant differences between salinities ($^{**}P < 0.01$ and $^{***}P < 0.001$) by Student's *t* test

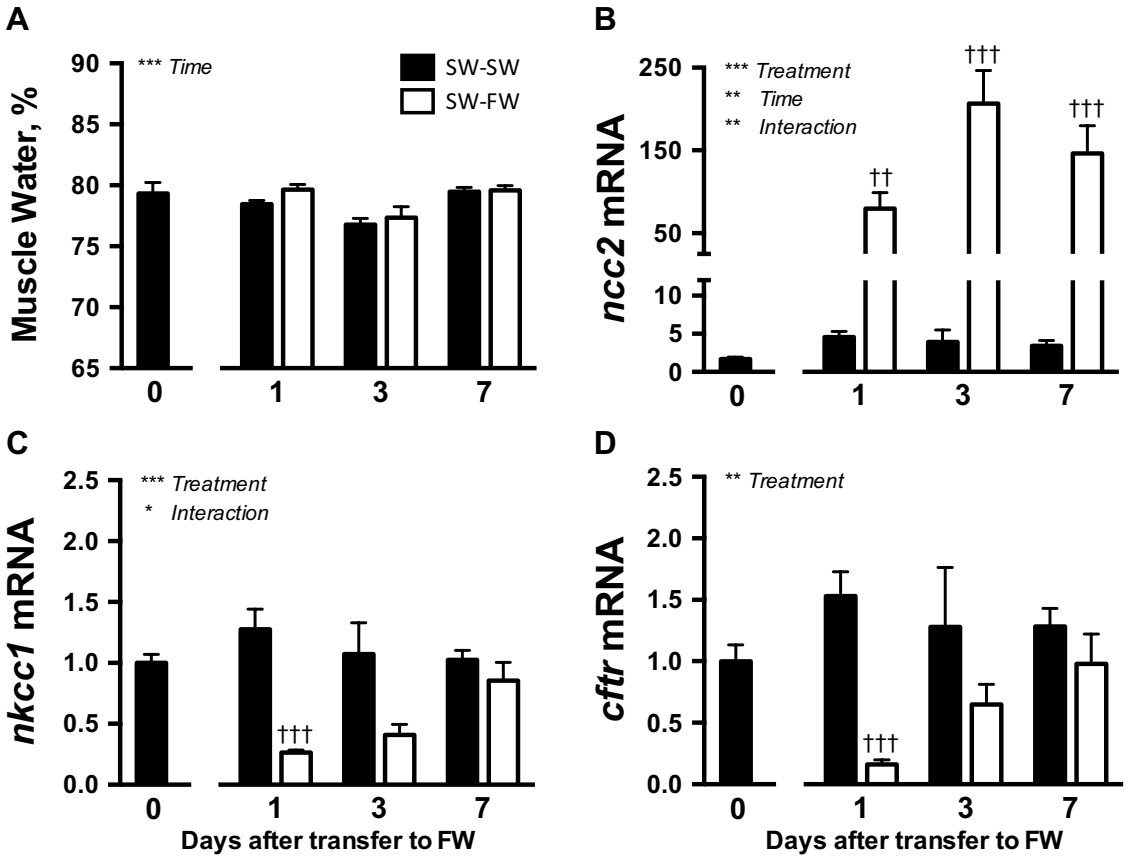

Fig. 3 Muscle water content (**a**) and *ncc2* (**b**), *nkcc1* (**c**), and *cftr* (**d**) mRNA levels in opercular epithelium at 1, 3, and 7 days after transfer of mummichogs from seawater (SW) to freshwater (FW; open bars). Mean ± SEM ($n = 6–8$). Time-matched control fish were maintained in SW (solid bars). Gene expression is presented as a fold change from time 0. Differences among groups were evaluated by two-way ANOVA. Significant effects of treatment, time, or an interaction are indicated in the respective panels ($^{*}P < 0.05$, $^{**}P < 0.01$, and $^{***}P < 0.001$). When there was a significant treatment effect, post hoc comparisons (Bonferroni's multiple comparisons test of time-matched groups) were made at each time point ($^{\dagger\dagger}P < 0.01$ and $^{\dagger\dagger\dagger}P < 0.001$)

Tissue and steady-state gene expression of *ncc2*, *nkcc1*, and *cftr*

We first determined the relative amounts of *ncc2* mRNA across tissues collected from FW-acclimated mummichogs. *ncc2* was highly expressed in opercular epithelium and gill, with markedly lower expression in the other examined tissues (Fig. 2a). In both the opercular epithelium and gill, *ncc2* levels exhibited markedly higher expression in long-term FW- versus SW-acclimated mummichogs (Fig. 2b, c). When we compared *nkcc1* and *cftr* levels between SW- and FW-acclimated animals, we only detected a significant difference in branchial *cftr* levels (Fig. 2d–g).

Effect of transfer from SW to FW on muscle water content and transporter gene expression in opercular epithelium and gill

There was a significant effect of time on muscle water content, but no effect of treatment or an interaction (Fig. 3a). Following transfer from SW to FW, there were significant main effects of treatment, time, and an interaction on *ncc2* levels in opercular epithelium (Fig. 3b). In animals transferred to FW, *ncc2* levels were elevated above time-matched (SW–SW) controls at 1, 3, and 7 days after transfer. For *nkcc1*, there was a significant main effect of treatment and an interaction with time; *nkcc1* levels were diminished at

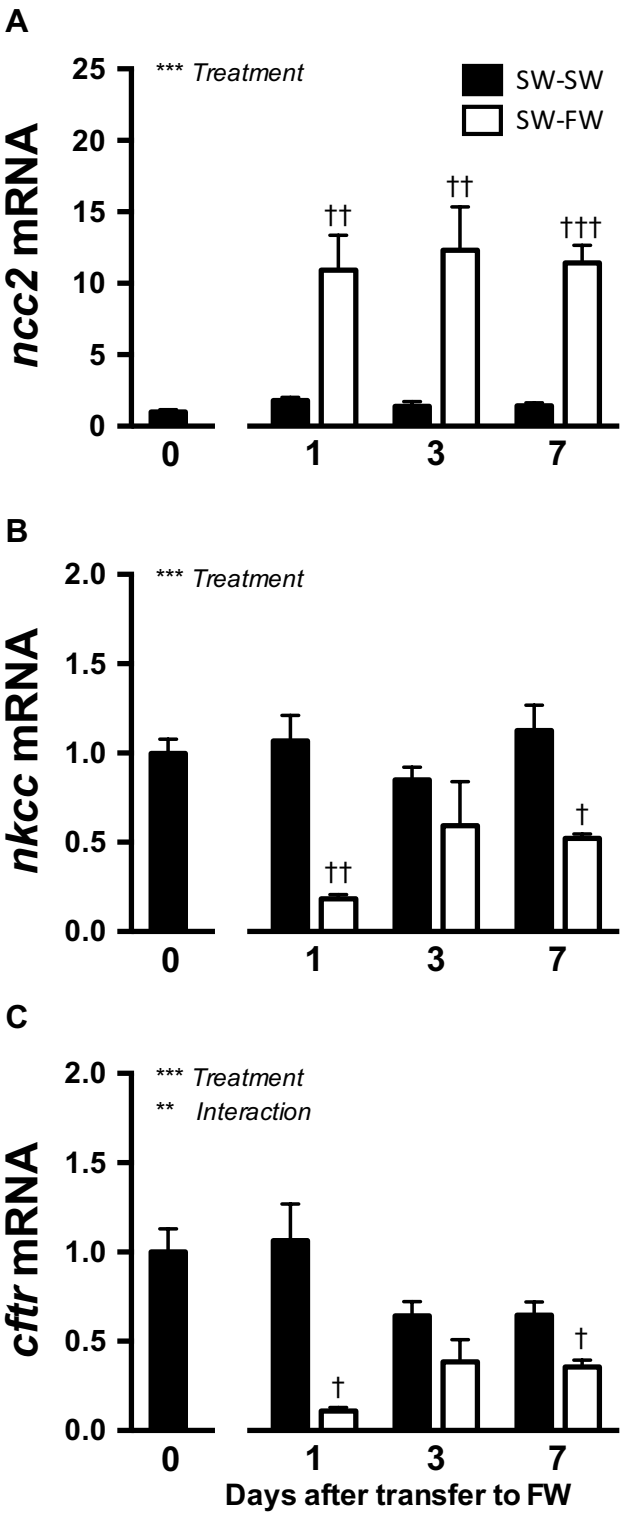

Fig. 4 Branchial *ncc2* (**a**), *nkcc1* (**b**), and *cftr* (**c**) mRNA levels at 1, 3, and 7 days after transfer of mummichogs from seawater (SW) to freshwater (FW; open bars). Mean ± SEM ($n = 6$–8). Time-matched control fish were maintained in SW (solid bars). Gene expression is presented as a fold change from time 0. Differences among groups were evaluated by two-way ANOVA. Significant effects of treatment, time, or an interaction are indicated in the respective panels (**$P < 0.01$ and ***$P < 0.001$). When there was a significant treatment effect, post hoc comparisons (Bonferroni's multiple comparisons test of time-matched groups) were made at each time point ($^{\dagger}P < 0.05$, $^{\dagger\dagger}P < 0.01$, and $^{\dagger\dagger\dagger}P < 0.001$)

1 day after transfer to FW (Fig. 3c). There was a significant main effect of treatment on *cftr* with diminished expression at 1 day after transfer to FW (Fig. 3d).

In the gill, there was a significant effect of treatment on *ncc2* levels following transfer from SW to FW (Fig. 4a). Similar to the pattern in the opercular epithelium, branchial *ncc2* levels were elevated above time-matched controls at 1, 3, and 7 days after transfer. For *nkcc1*, there was a significant effect of treatment (Fig. 4b), and for *cftr*, there was a significant effect of treatment and an interaction with time (Fig. 4c). Both *nkcc1* and *cftr* levels were diminished from time-matched controls at 1 and 7 days.

Effect of transfer from FW to SW on muscle water content and transporter gene expression in opercular epithelium and gill

There was a significant effect of time and an interaction with treatment on muscle water content; a modest increase in water content from controls (FW–FW) occurred at 1 day after transfer to SW (Fig. 5a). In the opercular epithelium, there was a significant main effect of treatment on *ncc2* with decreased levels compared to time-matched controls at 1 and 7 days after transfer (Fig. 5b). For both *nkcc1* and *cftr* there was a significant effect of treatment and time with both transcripts elevated at 1 day after transfer to SW (Fig. 5c, d).

There were significant treatment and interaction effects on branchial *ncc2* following transfer to SW (Fig. 6a). Branchial *ncc2* levels were diminished at 1 day after transfer. Transfer to SW resulted in significant effects of treatment, time, and an interaction on branchial *nkcc1* and *cftr* levels (Fig. 6b, c). Both transcripts were elevated above the time-matched controls at all time points.

Western blotting analysis

Western blots of crude gill membrane fractions probed with Ncc2 antibody revealed immunoreactive bands with apparent molecular mass ~ 68–70 kDa (Fig. 7a). Antibody neutralization with 400-fold molar excess of the antigenic peptide blocked the main immunoreactive band. This range is similar to the 75 kDa protein mass from the mummichog *ncc2* sequence (XM_021310632.1) deposited as part of BioProject (PRJNA286680) in the NCBI BioProject database, https://www.ncbi.nlm.nih.gov/bioproject. Quantification revealed a significant effect of environmental salinity on protein levels in gill and opercular epithelium. There were no tissue or interaction effects

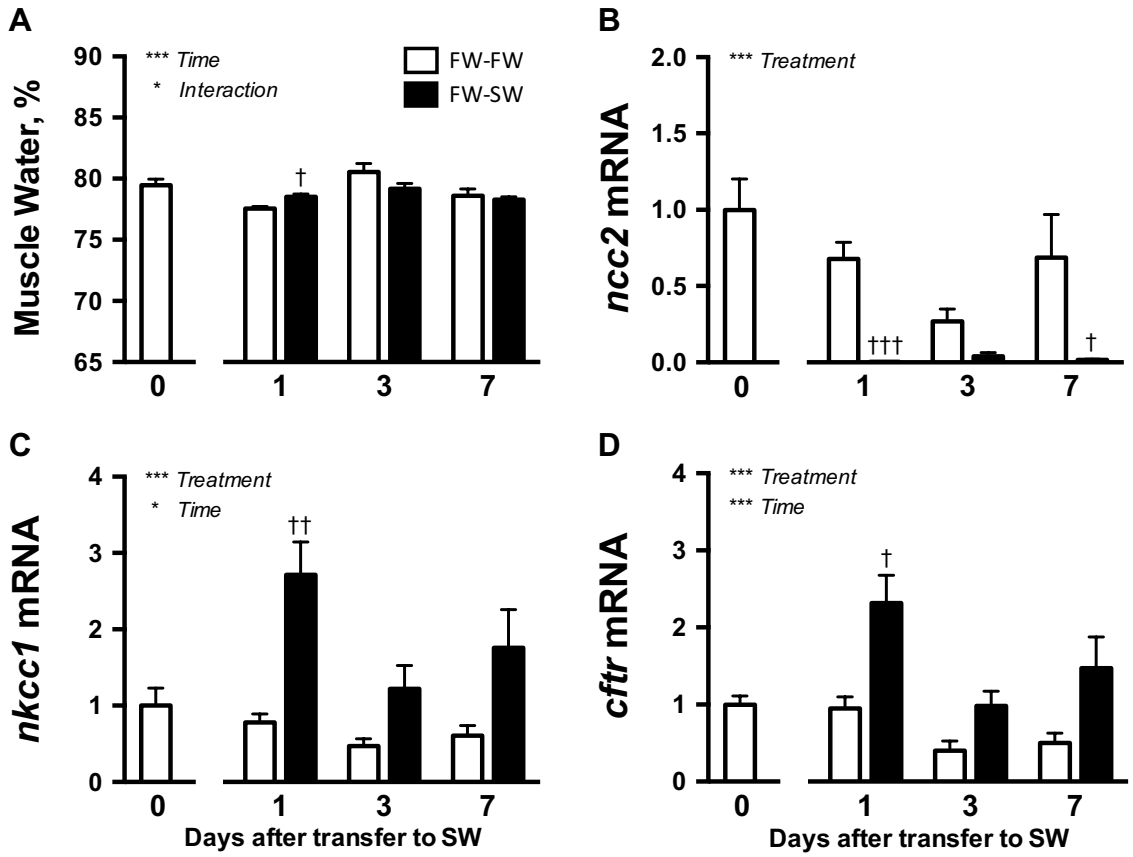

Fig. 5 Muscle water content (**a**) and *ncc2* (**b**), *nkcc1* (**c**), and *cftr* (**d**) mRNA levels in opercular epithelium at 1, 3, and 7 days after transfer of mummichogs from freshwater (FW) to seawater (SW; solid bars). Mean ± SEM ($n = 8$). Time-matched control fish were maintained in FW (open bars). Gene expression is presented as a fold change from time 0. Differences among groups were evaluated by two-way ANOVA. Significant effects of treatment, time, or an interaction are indicated in the respective panels ($^{*}P < 0.05$ and $^{***}P < 0.001$). When there were significant treatment or interaction effects, post hoc comparisons (Bonferroni's multiple comparisons test of time-matched groups) were made at each time point ($^{\dagger}P < 0.05$, $^{\dagger\dagger}P < 0.01$, and $^{\dagger\dagger\dagger}P < 0.001$)

meaning that protein abundance was not significantly different between tissues and the effect of salinity was the same across tissues (Fig. 7b).

Immunofluorescence microscopy

Ncc2-immunoreactivity was detected within Nka-positive ionocytes of the opercular epithelium of FW-acclimated mummichogs (Fig. 8a). In ionocytes exhibiting Ncc2- and Nka-immunoreactivity, Ncc2-immunoreactivity was located at the apical region of ionocytes as demonstrated by *z*-stack images (Fig. 8b–d). While Ncc2-immunoreactivity occurred within Nka-positive ionocytes, not all Nka-positive cells exhibited Ncc2-immunoreactivity (Fig. 8a). Ncc2-immunoreactivity in the opercular epithelium was abolished by preabsorbing the antibody with the synthetic antigen (Fig. 8e, f).

Discussion

Our collective results suggest that mummichogs employ Ncc2-expressing ionocytes for the uptake of ions from dilute environments. We identified an *ncc2* transcript expressed in a salinity-dependent fashion in both the opercular epithelium and gill. *ncc2* levels were modulated following salinity transfers, and thus we propose that concerted expression of *ncc2*, *nkcc1*, and *cftr* underlies the broad salinity tolerance of mummichogs. As a first step, we assessed the distribution of *ncc2* across tissues collected from FW-acclimated mummichogs. Consistent with the robust populations of ionocytes found in both tissues (Marshall et al. 1997), we observed strong *ncc2* expression in opercular epithelium and gill (Fig. 2a). The low *ncc2* levels observed in the kidney are consistent with Ncc1 (Slc12a3) mediating the reabsorption of Na^+ and Cl^- that

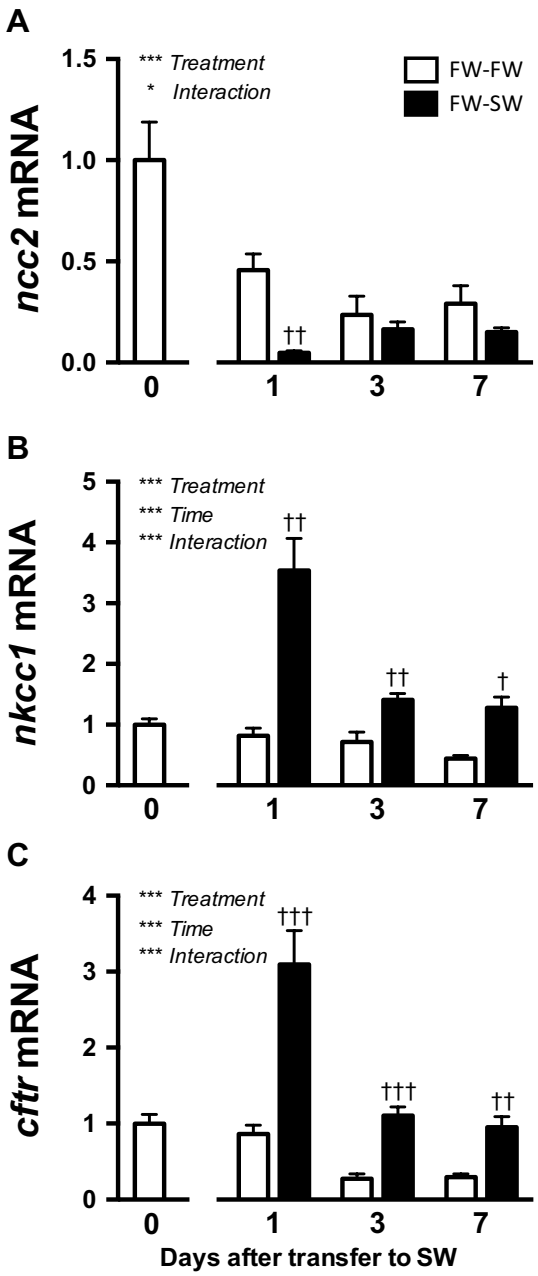

Fig. 6 Branchial *ncc2* (**a**), *nkcc1* (**b**), and *cftr* (**c**) mRNA levels at 1, 3, and 7 days after transfer of mummichogs from freshwater (FW) to seawater (SW; solid bars). Mean ± SEM ($n = 8$). Time-matched control fish were maintained in FW (open bars). Gene expression is presented as a fold change from time 0. Differences among groups were evaluated by two-way ANOVA. Significant effects of treatment, time, or an interaction are indicated in respective panels ($^{*}P < 0.05$ and $^{***}P < 0.001$). When there was a significant treatment effect, post hoc comparisons (Bonferroni's multiple comparisons test of time-matched groups) were made at each time point ($^{\dagger}P < 0.05$, $^{\dagger\dagger}P < 0.01$, and $^{\dagger\dagger\dagger}P < 0.001$)

occurs in distal tubules (Kato et al. 2011; Teranishi et al. 2013). In euryhaline species for which Ncc2-expressing ionocytes are critical to Na^+ and Cl^- uptake, *ncc2* levels are expressed in an inverse fashion to *nkcc1* and *cftr* which are expressed within SW-type (ion-secretory) ionocytes (Hiroi et al. 2008; Breves et al. 2010; Hsu et al. 2014; Bollinger et al. 2016). We similarly employed salinity transfer paradigms to assess the relationships among transcripts encoding sub-cellular markers of ionocyte function. In both the FW- and SW-transfer paradigms, *ncc2* in the branchial epithelium and gill showed inverse dynamics as *nkcc1* and *cftr* (Figs. 3, 4, 5, 6). These patterns suggest that activation of ion uptake pathways (via transcription of *ncc2*) occurs in tandem with the attenuation of ion secretion (via decreased *nkcc1* and *cftr*) upon exposure to FW, and vice versa upon exposure to SW. It was intriguing that under steady-state conditions, SW- and FW-acclimated mummichogs did not differentially express *nkcc1* and *cftr* in the opercular epithelium (Fig. 2d, f), while *ncc2* exhibited a 130-fold difference in expression (Fig. 2b). *nkcc1* and *cftr* transcription presumably remained poised for a possible increase in environmental salinity. This pattern is consistent with the maintenance of SW-type ionocytes in a 'ready state' even when mummichogs inhabit FW (Karnaky 1986). Interestingly, we detected Ncc2 protein in SW-acclimated mummichogs (Fig. 7b) when *ncc2* mRNA levels are very low (Fig. 2b, c); future studies should localize Ncc2 in the gill and opercular epithelium of SW-acclimated mummichogs.

In the species studied to date, there is strong agreement between *ncc2* mRNA levels and the densities of Ncc2/*ncc2*-expressing ionocytes (Hiroi et al. 2008; Inokuchi et al. 2008; Wang et al. 2009; Hsu et al. 2014). In turn, we performed immunohistochemistry on opercular epithelium from animals that were long-term acclimated to FW when *ncc2* levels were ostensibly elevated (Fig. 2b). We observed that Nka-positive ionocytes in opercular epithelium expressed Ncc2 in the apical region (Fig. 8b–d) in accord with an ion-absorptive role for Ncc2 in FW. This pattern mirrors the T4-immunoreactivity reported by Marshall et al. (2017) in opercular epithelium of FW-acclimated mummichogs. The apical Ncc2-immunoreactivity seen here in mummichog ionocytes is also in strong agreement with the patterns of Ncc2-immunoreactivity in Type-II ionocytes/Ncc-cells of tilapia and medaka (*Oryzias latipes*) (Hiroi et al. 2008; Hsu et al. 2014). While our collective gene expression and immunohistochemical observations suggest that Ncc2-expressing ionocytes within opercular and branchial epithelia are key effectors of ion uptake, when these tissues were functionally assessed previously, their contributions to FW-acclimation were deemed minimal (Marshall et al. 1997; Patrick et al. 1997; Wood and Laurent 2003). For example, Marshall et al. (2017) suggested that 'some' active Na^+ (but not Cl^-) uptake occurs across opercular and branchial epithelia, while Patrick et al. (1997) argued that Cl^- is not absorbed across opercular and branchial epithelia and is rather obtained through

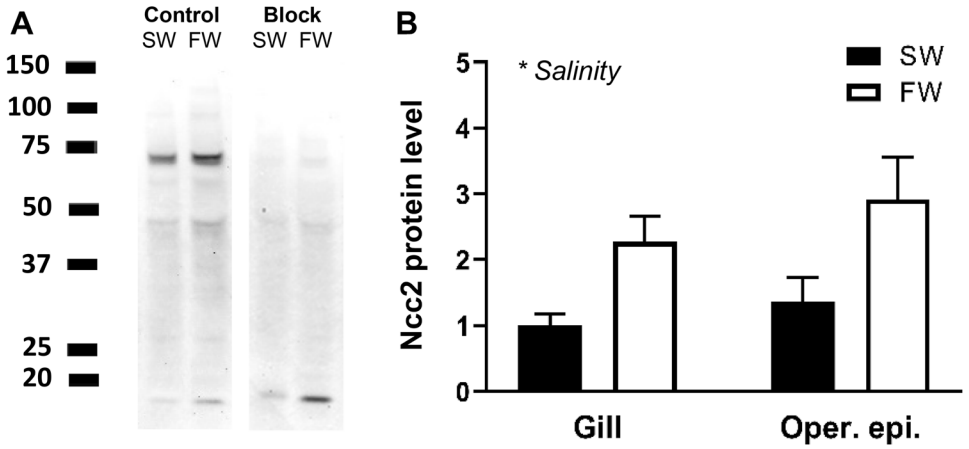

Fig. 7 Branchial and opercular membrane Ncc2 protein abundance in fish acclimated to SW or FW for 2 months. The Ncc2 antibody recognized immunoreactive proteins with an apparent molecular mass of 68–70 kDa in gill of SW- and FW-acclimated mummichogs (**a**, control) and the Ncc2 antibody was neutralized by 400-fold molar excess antigenic peptide prior to incubation (**a**, block). Abundance of Ncc2 is shown relative to branchial SW values ($n=4$–6) (**b**). Main (salinity and tissue) and interaction effects were evaluated by two-way ANOVA. There was only a significant effect of salinity ($^*P<0.05$)

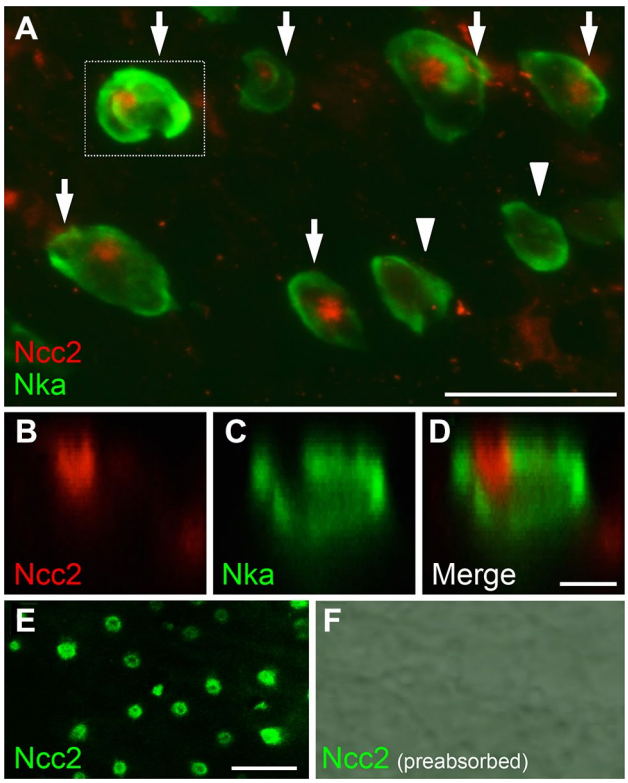

Fig. 8 Double immunofluorescent labeling of Ncc2 (red) and Nka (green) in opercular epithelium of FW-acclimated mummichog (**a**). Ncc2-immunoreactivity coincided with some Nka-positive ionocytes (arrows), while other Nka-positive ionocytes were not positive for Ncc2 (arrowheads). Scale bar = 15 µm. *xz*-scan of the ionocyte indicated by the dotted box labeled for Ncc2 (**b**) and Nka (**c**). Merged image of Ncc2 and Nka immunofluorescence showing apical Ncc2-immunoreactivity within ionocytes (**d**). Scale bar = 5 µm. Preabsorbing the antibody with the corresponding antigen abolished Ncc2-immunoreactivity (**e**, **f**). **f** Includes bright field to confirm the presence of opercular epithelium. Scale bar = 10 µm (colour figure online)

the diet. Under these scenarios, the fate of the Cl^- that is presumably cotransported with Na^+ by Ncc2 remains unclear. In zebrafish, Ncc2-cells express a member of the Clc family of Cl^- channels, namely Clc-2c, in the basolateral membrane that serves as a conduit for basolateral movement of Cl^- from the ionocyte interior into blood plasma (Pérez-Ruis et al. 2015; Wang et al. 2015). There is currently no information on whether mummichog ionocytes express one or more Clc-2/*clc-2* isoforms. If a basolateral conduit for Cl^- is not present, then it may help explain the lack of substantial Cl^- uptake by FW-acclimated mummichogs (Patrick et al. 1997; Patrick and Wood 1999; Wood and Laurent 2003).

The gill and opercular epithelium, especially with respect to *ncc2*, showed nearly identical transcriptional responses to salinity transfers. The matching transcriptional responses when considered alongside with the effect of salinity on Ncc2 protein levels in both tissues (Fig. 7b) suggest that functionally similar ionocytes operate in these tissues. Nonetheless, a quantification and comparison of the Ncc2-expressing ionocyte populations in branchial and opercular epithelium is required to more precisely infer whether Ncc2-dependent pathways in fact operate within both tissues. In clear contrast with *ncc2*, disparate patterns of *Na^+/H^+-exchanger* (*nhe2* and *-3*) expression occurred between branchial and opercular epithelium under both steady-state conditions and following salinity challenges (Scott et al. 2005). These patterns suggest differing capacities for ion uptake by Nhe2/3-dependent pathways between these tissues. Dymowska et al. (2012) proposed that branchial FW-type ionocytes co-express Nhe2 and Ncc2 in apical membrane. Thus, an important avenue for future work is to resolve whether Nhe2 and Ncc2 are actually co-expressed in mummichog ionocytes. Recall that not all Nka-positive cells exhibited Ncc2-immunoreactivity (Fig. 8a); thus, future

investigation is required to identify whether these cells express Nhe2/3. Regardless of whether Ncc2 and Nhe2/3 operate in a common FW-type ionocyte, the co-occurrence of multiple pathways for Na^+ uptake in mummichogs is reminiscent of patterns in zebrafish, where Nhe3b and Ncc2 play complementary roles in maintaining Na^+ homeostasis (Chang et al. 2013).

While the functional importance of the salinity-dependent *ncc2*/Ncc2 patterns described in this study remains to be clarified, this does not preclude a consideration of how extrinsic (salinity) and intrinsic (hormones) factors regulate *ncc2*/Ncc2. In euryhaline fishes, environmental osmotic/ionic conditions are important modulators of ion-transporting epithelia via the osmoreceptivity of ionocytes (Zadunaisky et al. 1995; Marshall et al. 2000, 2005, 2008; Flemmer et al. 2010; Kültz 2012). Indeed, *ncc2* levels in isolated branchial filaments of Mozambique tilapia were diminished by extracellular hyperosmotic conditions (Inokuchi et al. 2015). Thus, future work should investigate whether *ncc2* transcription and/or the post-translational regulation of Ncc2 (via with-no-lysine kinase 1) in mummichogs is sensitive to osmotic conditions (Marshall et al. 2017). As for a hormonal regulator of Ncc2- and/or Nhe2/3-dependent ion-uptake pathways in mummichog, prolactin is an obvious candidate given that it rescues the inability of hypophysectomized mummichogs to survive in FW (Burden 1956; Pickford and Phillips 1959). Our description of salinity-dependent expression of mummichog *ncc2*/Ncc2 in the current study enables us to now determine whether Ncc2 links prolactin with the FW adaptability of this historically important model in osmoregulatory physiology.

Acknowledgements We are grateful to Kirsten Tomlinson for collecting animals included in this report. We appreciate the excellent fish care provided by Kristin Salisbury, Aaron Cordiale, and Tracy Broderson. Jennifer Bonner and Eleanore Ritter provided valuable assistance with immunohistochemistry and confocal imaging.

Funding This study was supported by the National Science Foundation (IOS-1755131 to J.P.B and IOS-1251616 to C.K.T.), Arkansas Biosciences Institute (C.K.T) and Skidmore College (Start-Up Funds to J.P.B.).

Compliance with ethical standards

Conflict of interest The authors declare that they have no conflict of interest.

Ethical approval All applicable international, national, and/or institutional guidelines for the care and use of animals were followed.

References

Able KW (2002) Killifishes. In: Collette BB, Klein-MacPhee G (eds) Bigelow and Schroeder's fishes of the Gulf of Maine, 3rd edn. Smithsonian Institution Press, Washington, pp 292–297

Altschul SF, Madden TL, Schäffer AA, Zhang J, Zhang Z, Miller W, Lipman DJ (1997) Gapped BLAST and PSI-BLAST: a new generation of protein database search programs. Nucleic Acids Res 25:3389–3402

Benson DA, Karsch-Mizrachi I, Lipman DJ, Ostell J, Rapp BA, Wheeler DL (2000) GenBank. Nucleic Acids Res 28:15–18

Bollinger RJ, Madsen SS, Bossus MC, Tipsmark CK (2016) Does Japanese medaka (*Oryzias latipes*) exhibit a gill Na^+/K^+-ATPase isoform switch during salinity change? J Comp Physiol B 186:485–501

Brennan RS, Galvez F, Whitehead A (2015) Reciprocal osmotic challenges reveal mechanisms of divergence in phenotypic plasticity in the killifish *Fundulus heteroclitus*. J Exp Biol 218:1212–1222

Breves JP, Watanabe S, Kaneko T, Hirano T, Grau EG (2010) Prolactin restores branchial mitochondrion-rich cells expressing Na^+/Cl^- cotransporter in hypophysectomized Mozambique tilapia. Am J Physiol Regul Integr Comp Physiol 299:R702–710

Burden CE (1956) The failure of hypophysectomized *Fundulus heteroclitus* to survive in fresh water. Biol Bull 110:8–28

Burnett KG, Bain LJ, Baldwin WS, Callard GV, Cohen S, Di Giulio RT, Evans DH, Gómez-Chiarri M, Hahn ME, Hoover CA, Karchner SI, Katoh F, Maclatchy DL, Marshall WS, Meyer JN, Nacci DE, Oleksiak MF, Rees BB, Singer TD, Stegeman JJ, Towle DW, Van Veld PA, Vogelbein WK, Whitehead A, Winn RN, Crawford DL (2007) *Fundulus* as the premier teleost model in environmental biology: opportunities for new insights using genomics. Comp Biochem Physiol D 2:257–286

Chang WJ, Wang YF, Hu HJ, Wang JH, Lee TH, Hwang PP (2013) Compensatory regulation of Na^+ absorption by Na^+/H^+ exchanger and Na^+–Cl^- cotransporter in zebrafish (*Danio rerio*). Front Zool 10:46

Dymowska AK, Hwang PP, Goss GG (2012) Structure and function of ionocytes in the freshwater fish gill. Respir Physiol Neurobiol 18:282–292

Felsenstein J (1989) PHYLIP–Phylogeny Inference Package (version 3.2). Cladistics 5:164–166

Fiol DF, Kültz D (2007) Osmotic stress sensing and signaling in fishes. FEBS J 274:5790–5798

Flemmer AW, Monette MY, Djurisic M, Dowd B, Darman R, Gimenez I, Forbush B (2010) Phosphorylation state of the Na^+–K^+–Cl^- cotransporter (NKCC1) in the gills of Atlantic killifish (*Fundulus heteroclitus*) during acclimation to water of varying salinity. J Exp Biol 213:1558–1566

Griffith RW (1974) Environment and salinity tolerance in the genus *Fundulus*. Copeia 1974:319–331

Hiroi J, McCormick SD (2012) New insights into gill ionocyte and ion transporter function in euryhaline and diadromous fish. Respir Physiol Neurobiol 184:257–268

Hiroi J, Yasumasu S, McCormick SD, Hwang PP, Kaneko T (2008) Evidence for an apical Na–Cl cotransporter involved in ion uptake in a teleost fish. J Exp Biol 211:2584–2599

Hsu HH, Lin LY, Tseng YC, Horng JL, Hwang PP (2014) A new model for fish ion regulation: identification of ionocytes in freshwater- and seawater-acclimated medaka (*Oryzias latipes*). Cell Tissue Res 35:225–243

Inokuchi M, Hiroi J, Watanabe S, Lee KM, Kaneko T (2008) Gene expression and morphological localization of NHE3, NCC and NKCC1a in branchial mitochondria-rich cells of Mozambique tilapia (*Oreochromis mossambicus*) acclimated to a wide range of salinities. Comp Biochem Physiol A 151:151–158

Inokuchi M, Breves JP, Moriyama S, Watanabe S, Kaneko T, Lerner DT, Grau EG, Seale AP (2015) Prolactin 177, prolactin 188 and extracellular osmolality independently regulate the gene expression of ion transport effectors in gill of Mozambique tilapia. Am J Physiol Regul Integr Comp Physiol 309:R1251–1263

Karnaky KJ (1986) Structure and function of the chloride cell of *Fundulus heteroclitus* and other teleosts. Am Zool 26:209–224

Kato A, Muro T, Kimura Y, Li S, Islam Z, Ogoshi M, Doi H, Hirose S (2011) Differential expression of Na^+-Cl^- cotransporter and Na^+-K^+-Cl^- cotransporter 2 in the distal nephrons of euryhaline and seawater pufferfishes. Am J Physiol Regul Integr Comp Physiol 300:R284–R297

Katoh F, Cozzi RR, Marshall WS, Goss GG (2008) Distinct Na^+/K^+/$2Cl^-$ cotransporter localization in kidneys and gills of two euryhaline species, rainbow trout and killifish. Cell Tissue Res 334:265–281

Kültz D (2012) The combinatorial nature of osmosensing in fishes. Physiology 27:259–275

Lytle C, Xu JC, Biemesderfer D, Forbush B (1995) Distribution and diversity of Na–K–Cl cotransport proteins: a study with monoclonal antibodies. Am J Physiol 269:C1496–1505

Marshall WS, Grosell M (2006) Ion transport, osmoregulation and acid–base balance. In: Evans DH, Claiborne JB (eds) The physiology of fishes. CRC Press, Boca Raton, pp 177–230

Marshall WS, Bryson SE, Darling P, Whitten C, Patrick M, Wilkie M, Wood CM, Buckland Nicks J (1997) NaCl transport and ultrastructure of opercular epithelium from a freshwater-adapted euryhaline teleost, *Fundulus heteroclitus*. J Exp Zool 277:23–37

Marshall WS, Bryson SE, Luby T (2000) Control of epithelial Cl^- secretion by basolateral osmolality in the euryhaline teleost *Fundulus heteroclitus*. J Exp Biol 203:1897–1905

Marshall WS, Ossum CG, Hoffmann EK (2005) Hypotonic shock mediation by p38 MAPK, JNK, PKC, FAK, OSR1 and SPAK in osmosensing chloride secreting cells of killifish opercular epithelium. J Exp Biol 208:1063–1077

Marshall WS, Katoh F, Main HP, Sers N, Cozzi RR (2008) Focal adhesion kinase and β1 integrin regulation of Na^+, K^+, $2Cl^-$ cotransporter in osmosensing ion transporting cells of killifish, *Fundulus heteroclitus*. Comp Biochem Physiol A 150:288–300

Marshall WS, Cozzi RRF, Spieker M (2017) WNK1 and p38-MAPK distribution in ionocytes and accessory cells of euryhaline teleost fish implies ionoregulatory function. Biol Open 6:956–966

Patrick ML, Wood CM (1999) Ion and acid–base regulation in the freshwater mummichog (*Fundulus heteroclitus*): a departure from the standard model for freshwater teleosts. Comp Biochem Physiol A 122:445–456

Patrick ML, Pärt P, Marshall WS, Wood CM (1997) Characterization of ion and acid–base transport in the freshwater adapted mummichog (*Fundulus heteroclitus*). J Exp Zool 279:208–219

Pérez-Ruis C, Gaitán-Peñas H, Estévez R, Barrallo-Gimeno A (2015) Identification and characterization of the zebrafish ClC-2 chloride channel orthologs. Pflügers Arch 467:1769–1781

Pfaffl MW (2001) A new mathematical model for relative quantification in real-time RT-PCR. Nucl Acids Res 29(9):e45

Pickford GE, Phillips JG (1959) Prolactin, a factor in promoting survival of hypophysectomized killifish in fresh water. Science 130:454–455

Schultz ET, McCormick SD (2013) Euryhalinity in an evolutionary context. In: McCormick SD, Farrell AP, Brauner CJ (eds) Euryhaline fishes. Elsevier, New York, pp 477–529

Scott GR, Richards JG, Forbush B, Isenring P, Schulte PM (2004) Changes in gene expression in gills of the euryhaline killifish *Fundulus heteroclitus* after abrupt salinity transfer. Am J Physiol Cell Physiol 287:C300–C309

Scott GR, Claiborne JB, Edwards SL, Schulte PM, Wood CB (2005) Gene expression after freshwater transfer in gills and opercular epithelia of killifish: insight into divergent mechanisms of ion transport. J Exp Biol 208:2719–2729

Takei Y, Hiroi J, Takahashi H, Sakamoto T (2014) Diverse mechanisms for body fluid regulation in teleost fishes. Am J Physiol Regul Integr Comp Physiol 307:R778–792

Teranishi K, Mekuchi M, Kaneko T (2013) Expression of sodium/hydrogen exchanger 3 and cation-chloride cotransporters in the kidney of Japanese eel acclimated to a wide range of salinities. Comp Biochem Physiol A 164:333–343

Tipsmark CK, Mahmmoud YA, Borski RJ, Madsen SS (2010) FXYD-11 associates with Na^+-K^+-ATPase in the gill of Atlantic salmon: regulation and localization in relation to changed ion-regulatory status. Am J Physiol Regul Integr Comp Physiol 299:R1212–1223

Wang YF, Tseng YC, Yan JJ, Hiroi J, Hwang PP (2009) Role of SLC12A10.2, a Na–Cl cotransporter-like protein, in a Cl uptake mechanism in zebrafish (*Danio rerio*). Am J Physiol Regul Integr Comp Physiol 296:R1650–1660

Wang YF, Yan JJ, Tseng YC, Chen RD, Hwang PP (2015) Molecular physiology of an extra-renal Cl^- uptake mechanism for body fluid Cl^- homeostasis. Int J Biol Sci 11:1190–1203

Whitehead A (2010) The evolutionary radiation of diverse osmotolerant physiologies in killifish (*Fundulus* sp.). Evolution 64:2070–2085

Wood CM, Laurent P (2003) Na^+ versus Cl^- transport in the intact killifish after rapid salinity transfer. Biochim Biophys Acta 1618:106–119

Yan JJ, Hwang PP (2019) Novel discoveries in acid–base regulation and osmoregulation: a review of selected hormonal actions in zebrafish and medaka. Gen Comp Endocrinol 277:20–29

Zadunaisky JA, Cardona S, Au L, Roberts DM, Fisher E, Lowenstein B, Cragoe EJ, Spring KR (1995) Chloride transport activation by plasma osmolarity during rapid adaptation to high salinity of *Fundulus heteroclitus*. J Membr Biol 143:207–217